TURBULENT CROSSBAR IN NEAR-FIELD WITH PASSIVE SCALAR: EFFECT OF INITIAL CONDITION

N. Lefeuvre[1] & L. Djenidi[1] & R.A. Antonia[1]
[1] *University of Newcastle, NSW Australia,*

The velocity and passive scalar fields in the near-field behind a crossbar, made of two heated orthogonal square cylinders, are investigated with the aim to determine how the large scale structures, which are characteristics of this range, affect both the transport of the mean turbulent energy, q^2 ($\equiv u^2 + v^2 + w^2$ where u, v and w are the streamwise and the two lateral velocity components, respectively), and the scalar variance, θ^2. The assessment is performed through the second and third -order structure functions for both q^2 and θ^2.

The turbulent wake of the crossbar is simulated using the lattice Boltzmann method. The three dimensional computational domain is Cartesian and has $25D \times 10D \times 10D$ mesh points, D is the "diamter" of the bar. The mesh increments in the three directions are equal ($0.1D$). The crossbar is located at a distant of 5D from the inlet. Periodic boundary conditions are imposed on the lateral directions (y and z) and a zero longitudinal gradient is set at the outlet. A no-slip boundary condition is applied at the walls through a bounceback scheme and a constant velocity U_0 is applied at the inlet. More details on the LBM and the setup geometry can be found in [2]. The temperature is solved with the energy equation [3], coupled to the LBM solver. Heat is introduced by heating the crossbar with a constant temperature (T = 1 C). The Reynolds number based on U_0 and D is $Re_D = 1600$ and the Prandlt number is 0.75.

The distribution of the second order structure functions of $\langle(\delta q)^2\rangle$ ($\equiv \langle(\delta u)^2\rangle + \langle(\delta v)^2\rangle + \langle(\delta w)^2\rangle$) and $\langle(\delta\theta)^2\rangle$ ($\delta\alpha = \alpha(x+r) - \alpha(x)$, where $\alpha = u, v, w, \theta$) are shown in figure 1 and 2, respectively, for different downstream locations along the centerline. The structure functions are normalized by the Taylor λ and Corsin λ_θ microscale, $\langle q^2\rangle$ and $\langle\theta^2\rangle$:

$$\langle(\delta q*)^2\rangle = \langle(\delta q)^2\rangle \,/\, \langle q^2\rangle \tag{1}$$

$$\langle(\delta\theta*)^2\rangle = \langle(\delta\theta)^2\rangle \,/\, \langle\theta^2\rangle \tag{2}$$

Figure 1 shows that the large structures play an important role in the dynamics of $\langle(\delta q^*)^2\rangle$. Indeed, for $r > 10$, the oscillations seen on the structure functions are characteristic of the large coherent structures. $\langle(\delta q^*)^2\rangle$ reaches rapidly an equilibrium behind the cross bar for $r/\lambda < 10$ and $X/D > 16$. Antonia et al [1] report, a similar behavior in the fully develop range behind a gird ($X/M > 30$), where the turbulence is considered self-similar (red curve on figure 1).
Quite remarkably, $\langle(\delta\theta^*)^2\rangle$ presents a different behaviour to that of $\langle(\delta q^*)^2\rangle$ (figure 2), although the presence of the large coherent structures are also felt. Note that $\langle(\delta\theta^*)^2\rangle$ approaches the equilibrium state represented by Antonia et al [1] much slowly than $\langle(\delta q^*)^2\rangle$ does.
Further assessment of the small scale turbulence is currently in progress. The 2^{nd} order structure functions will be compared at different positions away from the centerline. Also, the scale-by-scale budget is currently evaluated and will be presented.

References

[1] R A Antonia, Smalley R J, Zhou T, Anselmet F, and Danaila L. Similarity solution of temperature structure functions in decaying homogeneous isotropic turbulence. *PhysicalL Review E*, 69, 2004.
[2] Lyazid Djenidi. Structure of a turbulent crossbar near-wake studied by means of lattice boltzmann simulation. *Phys. Rev. E*, 77, 2008.
[3] Reza H KHIABANI, Yogendra JOSHI, and Cyrus K. AIDUN. Heat transfer in microchannels with suspended solid particles: Lattice-boltzmann based computations. *Journal of heat transfer*, 132:124, 2010.

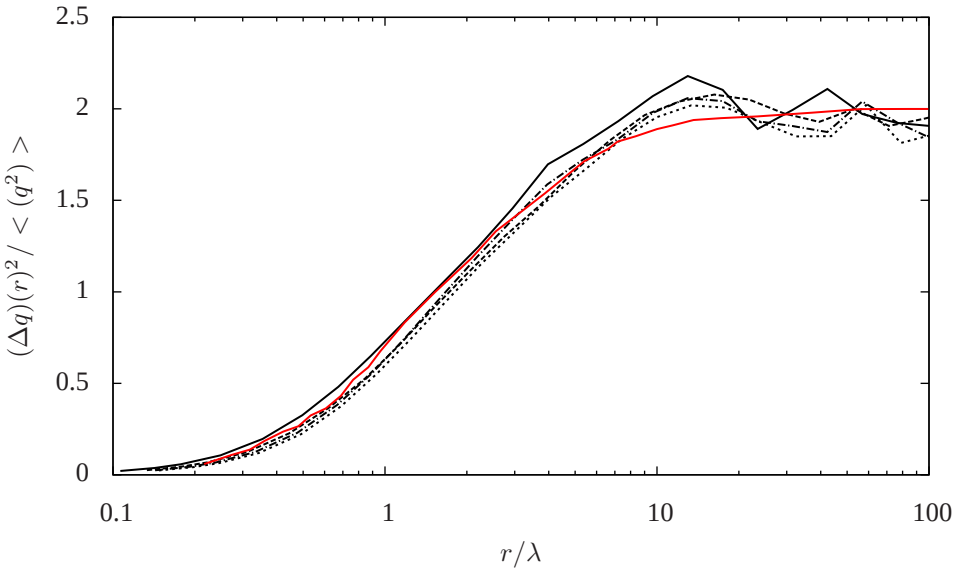


Figure 1. Distribution of $\left\langle (\delta q*)^2 \right\rangle$ vs r/λ. $X/D = 12$; solid line , $X/D = 16$; dashed line ,$X/D = 20$; dots-dash line and $X/D = 24$; dots line and Antonia et al (2004); red line.

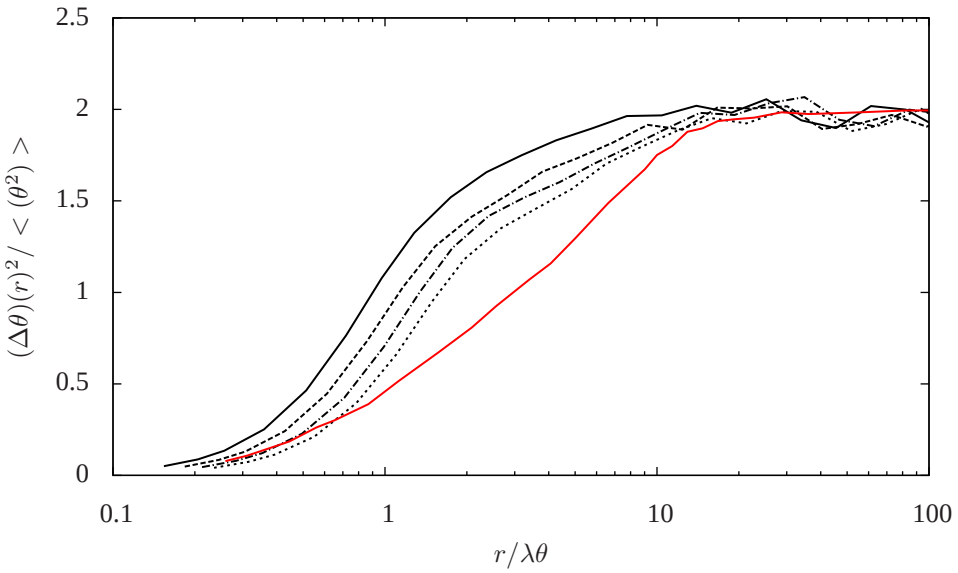


Figure 2. Distribution of $\left\langle (\delta \theta*)^2 \right\rangle$ vs r/λ_θ. $X/D = 12$; solid line , $X/D = 16$; dashed line ,$X/D = 20$; dots-dash line, $X/D = 24$; dots line and Antonia et al (2004); red line .